Microscopic Evidence of Spin State Order and Spin State Phase Separation in Layered Cobaltites $R\mathrm{BaCo_2O_{5.5}}$ with R = Y, Tb, Dy, and Ho

H. Luetkens,[1,*] M. Stingaciu,[2] Yu. G. Pashkevich,[3] K. Conder,[2] E. Pomjakushina,[2,4] A. A. Gusev,[3] K. V. Lamonova,[3] P. Lemmens,[5] and H.-H. Klauss[6]

[1]*Laboratory for Muon-Spin Spectroscopy, Paul Scherrer Institut, CH-5232 Villigen PSI, Switzerland*
[2]*Laboratory for Development and Methods, Paul Scherrer Institut, CH-5232 Villigen, Switzerland*
[3]*A. A. Galkin Donetsk Phystech NASU, 83114 Donetsk, Ukraine*
[4]*Laboratory for Neutron Scattering, Paul Scherrer Institut & ETH Zürich, CH-5232 Villigen, Switzerland*
[5]*IPKM, TU Braunschweig, D-38106 Braunschweig, Germany*
[6]*IFP, TU Dresden, D-01069 Dresden, Germany*

(Received 9 January 2008; published 2 July 2008)

We report muon-spin relaxation measurements on the magnetic structures of $R\mathrm{BaCo_2O_{5.5}}$ with R = Y, Tb, Dy, and Ho. Three different phases, one ferrimagnetic and two antiferromagnetic, are identified below 300 K. They consist of different ordered spin state arrangements of high-, intermediate-, and low-spin Co^{3+} of CoO_6 octahedra. Phase separation into well separated regions with different spin state order is observed in the antiferromagnetic phases. The unusual strongly anisotropic magnetoresistance and its onset at the FM-AFM phase boundary is explained.

DOI: 10.1103/PhysRevLett.101.017601 PACS numbers: 76.75.+i, 75.25.+z, 75.30.−m, 75.47.−m

Transition-metal oxides exhibit a rich variety of interesting properties like spin, orbital and charge order, giant magneto resistance (MR), and metal-insulator (MIT) transitions. These properties reflect electronic correlations and an interplay of partly competing degrees of freedom that may suppress long-range ordered states. Of special interest within this context are intrinsic and self-organized superstructures on microscopic length scales. Such inhomogeneous states may be induced by doping as in cuprates or manganites. However, chemical substitutions lead to considerable structural disorder that may impede the understanding of intrinsic correlation effects. The layered cobaltite $R\mathrm{BaCo_2O_{5.5}}$ (R denotes rare earth metal) is a prominent example among strongly correlated electron systems, where ordered electronic structures and unconventional transport phenomena exist without extrinsic doping and having all Co ions in the trivalent state [1–4]. Thereby, correlated phases with a minimum of structural disorder can be studied.

$R\mathrm{BaCo_2O_{5.5}}$ exhibits an orthorhombic crystal structure (*Pmmm*), which is derived from the basic perovskite by a doubling along the crystallographic b and c directions ($a_p \times 2a_p \times 2a_p$ unit cell, with a_p being the cell parameter of the cubic perovskite). The doubling of the b-axes originates from an alternation of CoO_5 square pyramids and CoO_6 octahedra along this direction, while the doubling along c is due to the layer stacking of $[\mathrm{BaO}][\mathrm{CoO_2}][R\mathrm{O_{0.5}}][\mathrm{CoO_2}]$ planes. In contrast to $LaCoO_3$, the octahedra and pyramids are heavily distorted [2,5,6]. These distortions support a variety of Co^{3+} spin states [low spin (LS, $S = 0$), intermediate spin (IS, $S = 1$), and high spin (HS, $S = 2$)] [7,8] as a function of crystallographic environment and temperature. A nonuniform spin state distribution or spin-state order (SSO) due to a complex interplay of electron-spin-orbital lattice degrees of freedom has been highlighted recently for $R\mathrm{BaCo_2O_{5.5}}$ [9–12]. $R\mathrm{BaCo_2O_{5.5}}$ shows a series of phase transitions, namely, a MIT below T_{MI} in the paramagnetic (PM) phase, a PM to ferro(ferri)magnetic (FM) transition at T_C, a FM to antiferromagnetic (AFM1) at T_{N1} which is accompanied by the onset of strong anisotropic magneto-resistive effects, and a AFM1 to antiferromagnetic (AFM2) phase transition at T_{N2}. Various contradicting magnetic structures including different spin states of the Co^{3+} ions and also SSO have been proposed, based on neutron diffraction [5,12–14], macroscopic measurements [15], and theoretical models [16], but no consensus has been reached.

In this Letter, we report magnetic structures of four powder samples of $R\mathrm{BaCo_2O_{5+\delta}}$ with $\delta \approx 0.5$ and R = Y, Tb, Dy, and Ho determined by means of muon-spin relaxation (μSR). Our main result is that irrespective of the rare-earth-metal ion, a homogenous FM phase with ferrimagnetic SSO of IS and HS states develops through two first order phase transitions into phase separated AFM1 and AFM2 phases with different types of antiferromagnetic SSO. We argue that the SSO and the phase separation play a similar role as intrinsic inhomogeneities like doping do in cuprates and manganites. The specific SSO in this cobaltite is also responsible for its unusual transport properties.

Powder samples of $R\mathrm{BaCo_2O_{5+\delta}}$ were synthesized by conventional solid state reaction techniques and subsequent oxygen content adjustment. Details of the sample preparation and determination of the oxygen content δ with an accuracy of ± 0.01 can be found in Ref. [17].

The μSR technique utilizes positively charged μ^+ implanted at interstitial lattice sites that probe local magnetic fields via the μ^+ spin precession frequency, which can be

observed from homogenous phases that extend over at least tens to hundreds of unit cells. The amplitude of the precession signal is proportional to the volume fraction of the corresponding magnetic phase. Therefore, μSR is an ideal tool to investigate phase separation phenomena in magnetic materials, see, e.g., [18].

In Fig. 1, zero field (ZF) μSR time spectra and the corresponding Fourier analysis of $Y\mathrm{BaCo_2O_{5.49}}$ are shown for characteristic temperatures regimes. Below T_C, a well defined spontaneous μ^+ spin precession develops indicative for the long-range magnetic order in the FM state. Two different magnetic μSR signals are observed showing that two magnetically inequivalent interstitial lattice sites are occupied by the muons: one which is associated with the high oscillation frequency ω_{HF} and another with a low frequency ω_{LF} which is too strongly damped for the Y and Ho compounds, but measurable for Tb and Dy. The amplitude of the oscillating signal indicates that each of the two different sites is 50% occupied. Below T_{N1}, the μSR spectra change drastically and several superimposed oscillation frequencies are observed. Below T_{N2}, the complexity of the μSR spectrum increases further indicating even more magnetically inequivalent μ^+ sites. All data have been fitted directly in the time domain by a superposition of exponentially damped oscillations and a practically undamped $1/3$ fraction of the total observable asymmetry. The $2/3$ oscillating and $1/3$ undamped μSR signal fractions evidences the complete static magnetic ordering of the powder samples, since in a spatial average, only $2/3$ of the magnetic field components are perpendicular to the μ^+ spin and cause a precession [18].

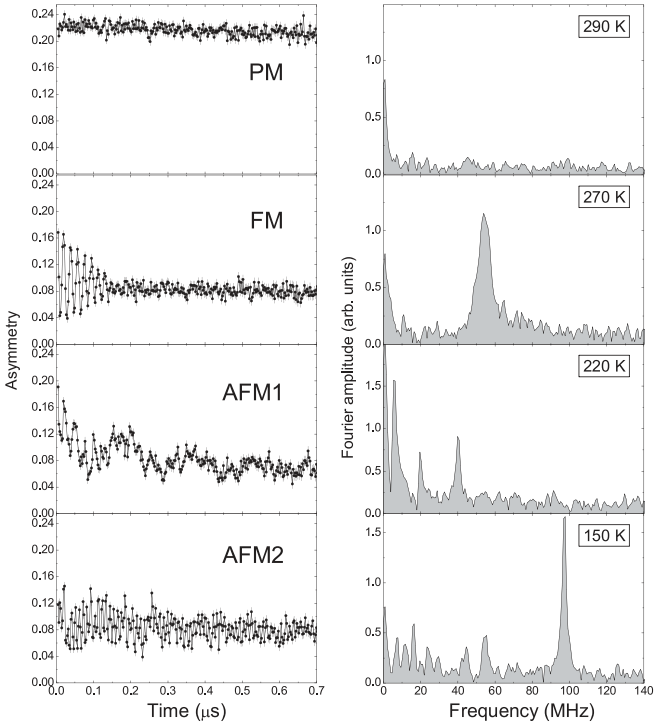

FIG. 1. Characteristic ZF $-$ μSR time spectra (left panel) and corresponding Fourier spectra (right panel) for temperatures within each of the different magnetic phases of $Y\mathrm{BaCo_2O_{5.49}}$.

The measured frequencies are displayed in Fig. 2 for all samples as a function of normalized temperature T/T_C. For clarity, the frequencies for the different magnetic phases (FM, AFM1, and AFM2) have been drawn in separate diagrams. The magnetic transition temperatures obtained from the μSR measurements are listed in Table I. Qualitatively and quantitatively, all samples show similar $\mu^+ SR$ frequencies indicating microscopically very similar magnetic structures, see Fig. 2. To evaluate quantitatively the consistency of the observed $\mu^+ SR$ frequencies with a specific magnetic structure model, the μ^+ position in the lattice has to be known. Therefore, electronic potential calculations have been performed using a modified Thomas—Fermi approach [19] and own structural data. This procedure has been verified on similar oxide crystal structures where experimentally determined μ^+ sites are available [20]. In $R\mathrm{BaCo_2O_{5.5}}$, two inequivalent μ^+ sites are obtained from the calculations which are located at

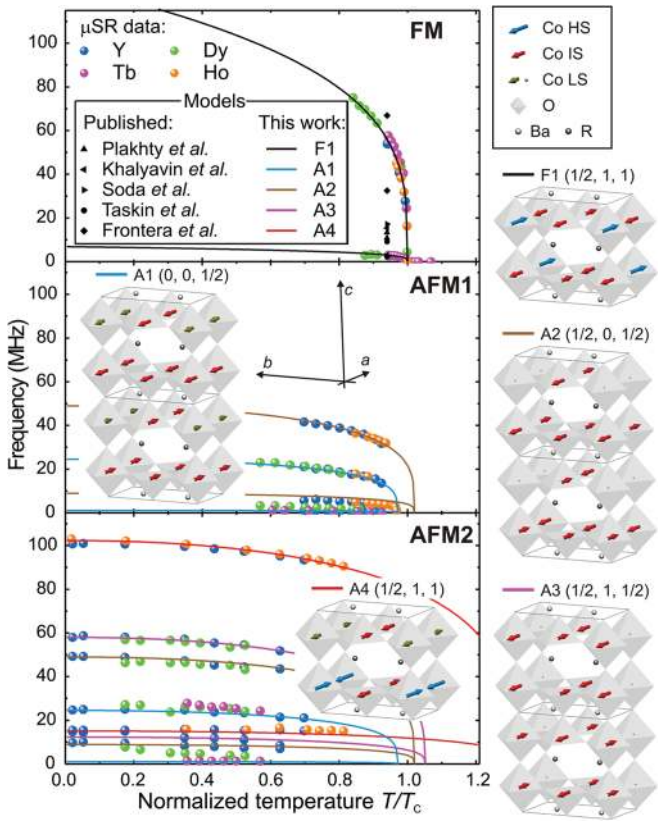

FIG. 2 (color). Muon-spin precession frequencies as a function of normalized temperature T/T_C for $R\mathrm{BaCo_2O_{5+\delta}}$ with R = Y, Tb, Dy, and Ho with $\delta \approx 0.5$. The solid lines present the fit or calculation for Y for respective magnetic structures, see text. Pairs of lines which fit with the same power law and belong to the same structure are drawn in the same color. Magnetic reflections above magnetic structures are given for the unit cell $a_p \times 2a_p \times 2a_p$. For the FM phase, the expected frequencies for various magnetic structures [5,13–16] have been calculated for $T = 0.94T_C$, see text.

TABLE I. Magnetic transition temperatures obtained by ZF − μSR for RBaCo$_2$O$_{5+\delta}$ with R = Y, Tb, Dy, and Ho.

	Y^{3+}	Tb^{3+}	Dy^{3+}	Ho^{3+}
δ	0.49(1)	0.50(1)	0.50(1)	0.47(1)
T_C (K)	287(1)	281(1)	285.5(1.0)	283(0.5)
T_{N1} (K)	267(3)	262(3)	245(10)	273.5(0.5)
T_{N2} (K)	200(5)	165(5)	155(5)	235(5)

$N1 = (0, 0.36, 0)$ and $N2 = (0.31, 0, 0)$ positions in the *Pmmm* crystal structure, i.e., about 1 Å away from apical oxygens in the BaO-plane. These are typical sites, which have also been found, e.g., in high-T_C cuprate superconductors [21].

For a given magnetic structure to be tested for consistency with the μSR data, the local magnetic dipole fields at the two μ^+ sites can be calculated numerically. Since there are two μ^+ sites in the lattice, two different μSR frequencies are calculated for a homogenous phase. These two frequencies show a typical ratio which is characteristic for the magnetic structure due to the symmetries of their corresponding μ^+ sites. Additionally, they have to display the same T dependence. Finally, the magnetic model has to reproduce the magnetic Bragg peaks that have been detected in neutron diffraction studies [5,12,14,22–24], which strongly reduces the number of structures to be tested.

The magnetic structure which is able to consistently describe the observed μSR frequencies in FM phase is a checkerboard-like HS-IS AFM SSO on the octahedral sites with IS AFM order on the pyramids and all moments pointing along the crystallographic a-axis, see the F1 structure in Fig. 2. The T dependence of the two frequencies observed in the FM phase can be perfectly described by the same power law $\omega(T) = \omega(0)[1 - (T/\gamma T_C)^\alpha]^\beta$ with $\omega_{HF}(0) = 127.7$ MHz, $\omega_{LF}(0) = 6.9$ MHz, $\alpha = \gamma = 1$, and $\beta = 0.290(5)$. This is reproduced by the dipole field calculation by using the zero temperature HS and IS values $M_0^{\rm oct}$ as listed in Table II for the magnetic moments of Co in the two octahedral sites and $M_0^{\rm pyr} = 2\mu_{\rm B}$ (IS) on the pyramidal site. The calculation is shown as a solid black line in Fig. 2. The exponent $\beta = 0.290(5)$ points to a 3D-Ising character of the interactions consistent with the observed Ising-like anisotropy [15,25,26]. The ferrimagnetic model F1 is compatible with neutron scattering results [5,12,14,23,24] since it conforms to the most intense (1/2, 1, 1) magnetic reflection. The structural doubling along the a-axis and the onset of *Pmma* symmetry below MIT as observed in Gd [27] by x ray and in Dy [24] by neutron diffraction studies is also naturally obtained by this magnetic structure, since the alternating IS and HS Co^{3+} with different ionic radii modulate the structure accordingly.

TABLE II. Magnetic moments $m^{\rm oct}(T) = M_0^{\rm oct}(1 - (T/\gamma T_C)^\alpha)^\beta$ of the two different octahedral Co for R = Y which are used for the calculation of the colored lines in Fig. 2. In all phases, the pyramidal Co are in the IS state with $M_0^{\rm pyr} = 2\mu_{\rm B}$. The corresponding most intense magnetic Bragg reflection is also listed.

Phase	Reflection	$M_0^{\rm oct}/\mu_{\rm B}$	$M_0^{\rm oct}/\mu_{\rm B}$	α	β	γ
F1	(1/2,1,1)	4.4 (HS)	2.2 (IS)	1.0	0.290(5)	1.00
A1	(0,0,1/2)	1.7 (IS)	0.3 (LS)	2.2	0.26(1)	0.97
A2	(1/2,0,1/2)	2 (IS)	0 (LS)	2.2	0.26(1)	1.02
A3	(1/2,1,1/2)	2 (IS)	0 (LS)	2.2	0.29(1)	1.05
A4	(1/2,1,1)	4.1 (HS)	1.2 (LS)	2.2	0.29(1)	1.30

Several previously proposed models for the FM phase have also been examined by calculating the magnetic dipole fields at the two μ^+ sites. We ensured that all models give the same net magnetization of $0.5\mu_B$/F.U. for single crystals, i.e., approximately $0.25\mu_B$/F.U. for powders at $T = 0.94T_C$, by scaling the local moments for the magnetic models [5,13–16]. None of the published models is close to the observed μSR frequencies, see Fig. 2. In particular, none of the models exhibits the correct ratio of the two fields at the two μ^+ sites, which is independent on the scaling.

In the AFM phases, more than two μSR frequencies are observed. Yet, these frequencies always appear in pairs of one HF and one LF signal whose T dependence can be fitted with the same power law, while the other pairs follow different laws. Each pair of fitted lines is shown with a unique color in Fig. 2 (only the fit for the Y compound is shown). Therefore, we conclude that every pair of μSR signals belongs to a separate magnetic phase with a different T dependence of its order parameter and different extrapolated Néel temperatures ($T_N^* = \gamma T_C$). A clear μSR precession with a small spread of dipole fields is obtained only if the volume of a homogenous phase extends over at least tens to hundreds of unit cells. Thus, we conclude that the first order FM-AFM1 phase transition in layered cobaltites occurs with a phase separation, i.e., with simultaneous appearance of phases with different magnetic structures and different types of SSO.

Depending on R, we deduce two types of SSO (A1 and A2) in the AFM1 phase and up to four different types of SSO (A1–A4) in the AFM2 phase, which appear at the respective phase transitions and develop on the cost the high temperature phases when the temperature is lowered. The magnetic structures for all phases of the Y compound are shown in Fig. 2. Their deduced sublattice magnetic moments and T dependence are listed in Table II. A common feature of all structures is the AFM coupling of IS states on pyramidal sites along the c-direction. The stability of pyramidal IS states in RBaCo$_2$O$_{5.5}$ has recently been revealed by *ab initio* calculations [28]. Note that the structures A1–A3 present just a different topology of the IS/LS pair distribution on neighboring octahedral sites which have very similar self-energy. Probably, this is the

reason of the phase separation at the FM-AFM1 phase transition. The representative magnetic reflections of the structures F1 and A1–A4 are given in Table II. All have been observed by neutron diffraction [5,22–24] in the corresponding phases, but were not or differently assigned. Only the phase A3 has also been deduced from one neutron study [12]. Phase separation can be identified by a volume sensitive local probe like μSR or NMR. The observed low temperature AFM SSO phase separation with IS states on pyramids and with IS and LS (A1–A3) and HS (A4) states on octahedra is consistent with the low temperature NMR study of the Y compound [29], where four different types of Co species have been detected.

Now, we discuss some consequences of the observed magnetic structures. Antiferromagnetic coupling in pyramids along c-axis is the main motive of all structures (F1 and A1–A4). This is in accordance with Goodenough-Kanamori-Anderson (GKA) rules for IS ($t_{2g}^5 e_g^1$) states on pyramids with the e_g-electrons occupying either the $3z^2 - r^2$ or the $x^2 - y^2$ orbitals. Furthermore, one can show that all magnetic bonds in the A1–A4 structures fulfill GKA rules (assuming a certain occupancy of the orbitals). On the other hand, GKA rules can not be satisfied for the F1 HS-IS SSO structure realized in the FM state, where one of the pyramid-octahedra magnetic bonds remains frustrated in the G-type order. This frustration might explain the narrow temperature range in which FM order is observed.

Finally, the detected magnetic structures are able to explain qualitatively the transport properties of $R\mathrm{BaCo_2O_{5.5}}$ in a localized picture of charge carriers motion [30]. The A1 phase consists of ferromagnetic ab-planes of Co^{3+} in IS states along which "electron" (HS Co^{2+} species, $t_{2g}^5 e_g^2$) hopping is allowed, while it is impossible along c-axis for all A1–A4 phase due to the so-called spin blockade mechanism [30,31]. Less pronounced "hole" (LS Co^{4+} species, t_{2g}^5) hopping is allowed through the channels of LS states along a-axis in the A1 and A2 phases and along c-axis in the A3 phase. This explains the 1 order of magnitude different resistivities along c- and a-axis in detwinned single crystals of $\mathrm{EuBaCo_2O_{5.5}}$ [32]. The phase separation into less and more conductive phases in $R\mathrm{BaCo_2O_{5.5}}$ leads to a resistivity behavior similar to low doped manganites where conductive and isolating regions coexist. Also, the observed strong anisotropy of the MR [26] can be understood on the basis of the deduced magnetic structures. Because of the Ising-like anisotropy a magnetic field along the a-axis may switch the weakly AFM coupled neighboring FM planes in the A1 phase to the FM alignment (as in usual metamagnetic antiferromagnets) making "electron" transport along c possible. As a result, a very large MR for fields along a is observed. Furthermore, the hopping process for both kinds of charge carriers is strictly prohibited in the F1 phase, even when the magnetic structure is canted by a magnetic field, which explains the unusual onset of the MR phenomenon below T_{N1}.

In conclusion, we present the first local probe (μSR) investigation on the magnetic structures of the $R\mathrm{BaCo_2O_{5+\delta}}$ system with $\delta \approx 0.5$. SSO is established in all magnetic phases. Phase separation into well separated regions with different SSO is observed in the AFM phases. The deduced SSO magnetic structures are consistent with the magnitude of the magnetoresistance, its unusual anisotropy, and its onset at the FM-AFM phase boundary.

This work was performed at the Swiss Muon Source, Paul Scherrer Institut, Villigen, Switzerland. We acknowledge support by DFG, ESF-HFM, and the NCCR MaNEP project.

*hubertus.luetkens@psi.ch

[1] A. A. Taskin, A. N. Lavrov, and Y. Ando, Phys. Rev. B **71**, 134414 (2005).
[2] Y. Moritomo *et al.*, Phys. Rev. B **61**, R13325 (2000).
[3] A. Maignan *et al.*, J. Solid State Chem. **142**, 247 (1999).
[4] D. Akahoshi and Y. Ueda, J. Phys. Soc. Jpn. **68**, 736 (1999).
[5] V. P. Plakhty *et al.*, Phys. Rev. B **71**, 214407 (2005).
[6] E. Pomjakushina, K. Conder, and V. Pomjakushin, Phys. Rev. B **73**, 113105 (2006).
[7] H. Wu, Phys. Rev. B **64**, 092413 (2001).
[8] E. S. Zhitlukhina *et al.*, J. Phys. Condens. Matter **19**, 156216 (2007).
[9] M. Coutanceau *et al.*, Solid State Commun. **96**, 569 (1995).
[10] D. Foerster *et al.*, Phys. Rev. B **64**, 075104 (2001).
[11] D. I. Khomskii and U. Low, Phys. Rev. B **69**, 184401 (2004).
[12] F. Fauth, E. Suard, V. Caignaert, and I. Mirebeau, Phys. Rev. B **66**, 184421 (2002).
[13] M. Soda *et al.*, J. Phys. Soc. Jpn. **72**, 1729 (2003).
[14] C. Frontera *et al.*, Phys. Rev. B **74**, 054406 (2006).
[15] A. A. Taskin, A. N. Lavrov, and Y. Ando, Phys. Rev. Lett. **90**, 227201 (2003).
[16] D. D. Khalyavin, Phys. Rev. B **72**, 134408 (2005).
[17] K. Conder *et al.*, Mater. Res. Bull. **40**, 257 (2005).
[18] P. D. de Reotier and A. Yaouanc, J. Phys. Condens. Matter **9**, 9113 (1997).
[19] I. M. Reznik, F. G. Vagizov, and R. Troc, Phys. Rev. B **51**, 3013 (1995).
[20] E. Holzschuh *et al.*, Phys. Rev. B **27**, 5294 (1983).
[21] H. H. Klauss, J. Phys. Condens. Matter **16**, S4457 (2004).
[22] M. Soda *et al.*, J. Phys. Soc. Jpn. **75**, 104706 (2006).
[23] D. D. Khalyavin *et al.*, Phys. Rev. B **75**, 134407 (2007).
[24] Y. P. Chernenkov *et al.*, Phys. Lett. A **365**, 166 (2007).
[25] D. D. Khalyavin *et al.*, Phys. Rev. B **67**, 214421 (2003).
[26] Z. X. Zhou and P. Schlottmann, Phys. Rev. B **71**, 174401 (2005).
[27] Y. P. Chernenkov *et al.*, Phys. Rev. B **71**, 184105 (2005).
[28] V. Pardo and D. Baldomir, Phys. Rev. B **73**, 165117 (2006).
[29] M. Itoh *et al.*, Physica B (Amsterdam) **329**, 751 (2003).
[30] A. Maignan *et al.*, Phys. Rev. Lett. **93**, 026401 (2004).
[31] A. A. Taskin and Y. Ando, Phys. Rev. Lett. **95**, 176603 (2005).
[32] Z. X. Zhou *et al.*, Phys. Rev. B **70**, 024425 (2004).